Electroreduction of oxygen on a (100)-like polycrystalline gold surface in an alkaline solution containing Pb(II)

Carlos Paliteiro *, Natércia Martins

Departamento de Química, Universidade de Coimbra, P-3049 Coimbra, Portugal

Abstract

In a previous work from this laboratory, it was shown that it is possible to electrochemically modify a polycrystalline surface of gold so that it behaves towards O_2 reduction like the (100) gold plane. To check whether this similarity in behavior is due to the presence on the (100)-like surface of sufficiently large (100) spots, the process of the upd of Pb(II) was used in this work as a probe of the surface crystallographic orientations both in deaerated and in O_2−saturated solutions. The observed cyclic voltammograms (CV) and polarization curves were entirely different from those reported in the literature for a typical polycrystalline gold surface. The CV data were analyzed in an attempt to gain insight on the crystallography of the (100)-like surface. The influence of adsorbed lead on the electroreduction of oxygen in 1 M NaOH on the (100)-like surface was also scrutinised. It was found that the reduction is differently affected by adsorbed Pb(II) ions and by underpotential deposited Pb adatoms. Adsorbed Pb(II) do not change the reduction mechanism, it only alters the rate constant for HO_2^- disproportionation, whereas the surface becomes able to reduce O_2 to OH^- without desorption of HO_2^- to the solution bulk when modified by Pb adatoms. The details of the electroreduction of O_2 and of HO_2^- are thoroughly discussed in relation to the surface processes underneath. Together with the CV data, they show that there are no significant (100) spots on the (100)-like surface and that this surface is structurally different from the gold (100) plane. © 1998 Elsevier Science Ltd. All rights reserved.

Keywords: Gold; Oxygen reduction; Lead upd; Modified surfaces; Electrocatalysis

1. Introduction

As showed recently [1], it is possible to electrochemically modify a polycrystalline gold surface (pc-Au) so that it behaves towards O_2 reduction both in $HClO_4$ and in alkaline solutions like a (100) plane, the most active surface found so far for the reaction in such media. In fact, in 1M NaOH for example, the onset potential for the reduction on the modified surface (hereafter called '100'-Au) is ≈50 mV more anodic than on pc-Au and the polarization curves show a maximum at ≈750 mV vs. the reversible hydrogen electrode (RHE) where the current approaches the 4-electron level.

It has been a challenge for us to understand why '100'-Au has such a catalytic activity, since it may lead to the identification of reaction sites (or surface structures) that will allow the tailoring of surfaces with adequate activity and stability for O_2 electroreduction. One may wonder, for example, whether the (100)-like behavior of the '100'-Au surface is due to the presence on it of patches of the (100) plane. One experimental approach to this problem is to examine the surface directly by applying in-situ STM [2]. Another approach is to use the upd of metals as a probe, since such a process is quite sensitive to surface structure. The upd of lead is a convenient example of this process because it was studied in detail on pc-Au and Au single crystals (mainly in $HClO_4$) so that a sort of atlas of lead upd spectra on most of the Au planes is available in the literature [3, 4]; data on the electroreduction

---

* Corresponding author.

of O_2 by pc-Au modified by lead upd are also available [5–9]. Since all this work is a good basis for comparison, we decided to look at the upd of lead on the '100'-Au surface and to investigate the influence of such deposit upon the reduction of O_2 and of HO_2^- in 1 M NaOH. The results obtained, which this paper reports and discusses, appear to show that the '100'-Au surface is structurally different from the (100) gold plane.

2. Experimental

The polycrystalline Au electrode used in this work was a disc of 99.99% Au from Johnson Matthey with a geometric area of 0.150 cm^2 and formed as a RDE with Teflon. The disc was polished with diamond paste to a 0.25 μm finish, sonicated in an ultrasonic bath and carefully cleaned with AnalaR ethanol and pyro-distilled water. The potential of this pc-Au surface was first scanned at 50 mVs^{-1} in a deaerated 0.5 M H_2SO_4 solution between the onsets of H_2 and of O_2 evolution, until the well-known stable cyclic voltammogram (CV) of gold in this acid solution was observed. A potential of −300 mV vs. RHE was then applied for 10 min with the RDE rotating at 10 rps. This applied potential assured a current density of about 670 μA cm^{-2}. After this pretreatment, the electrode was carefully washed with pyrodistilled water and put in a desiccator. Four days later the CVs and the polarization curves obtained on the pretreated electrode in a 1 M NaOH solution by scanning the potential between −100 mV and 1000 mV (i.e. by keeping the upper potential limit below 1150 mV, which is the stability anodic limit of '100'-Au) were characteristic of a '100'-Au surface [1]. We measured the real area of the polished pc-Au surface using Wood's method [10] (surface roughness = 1.4), but the relationship between this area and the real area of the final '100'-Au surface is uncertain.

$HClO_4$, NaOH and PbF_2 were of proanalysis or AnalaR quality. All solutions were prepared with pyrodistilled water. General purpose 30% H_2O_2 was distilled following the procedure given by Perrin et al. [11]; the fraction of pure H_2O_2 was collected and diluted with pyrodistilled water to obtain a 2.5 M stock solution. The H_2O_2 solutions for the experiments reported below were prepared from this stock solution just before use and the actual concentration of H_2O_2 was determined by titration with standardized $KMnO_4$.

An electrochemical cell with three-separated compartments was used. Solutions in this cell were saturated with high-purity O_2 (type C) or argon (N46) from Air Liquide. The potential of the Au electrode was controlled by a Pine Instruments AFRDE4 potentiostat and measured against a 1 M NaOH Hg/HgO

electrode or a standard calomel electrode (SCE); it is referred hereafter to the reversible hydrogen electrode (RHE). Working electrode rotation was provided by a Pine Instruments AFMSRX rotator. A glassy carbon rod was used as the counter electrode. All the experimental curves were recorded on a Philips PM 8043 *X–Y* recorder.

3. Results

3.1. UPD of lead on '100'-Au

Fig. 1(a) and (b) show the upd spectra of 1 mM Pb (II) recorded on '100'-Au, respectively in 0.01 M $HClO_4$ and in 1 M NaOH. Although the predominant Pb(II) species are hydrated Pb^{2+} in the acid solution and $HPbO_2^-$ in the alkaline, the shapes of the two spectra are similar and quite different from those reported for the (100) [3, 5, 6] and the pc-Au [12] surfaces. It is known that, on the Au surfaces and in acid, Pb(II) deposits at underpotential as a totally discharged Pb atom [3]. Given the similarity of the spectra, it is probable that the same happens in alkaline.

In 1 M NaOH + 1 mM Pb (II), the upd process starts at 600 mV, the upd spectrum is dominated by a broad peak at ≈450 mV, followed by a much smaller feature at ≈370 mV and a well defined peak at 300 mV (cf. Fig. 1(b)).
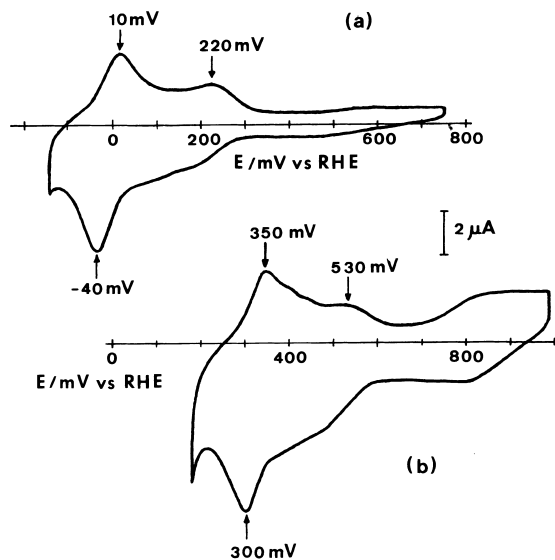

Fig. 1. CVs recorded at 20 mV s^{-1} and rotation rate of 9 s^{-1} on a '100'-Au surface in argon-saturated (a) 0.01 M $HClO_4$ + 1 mM Pb(II) and (b) 1 M NaOH + 1 mM Pb(II) solutions.
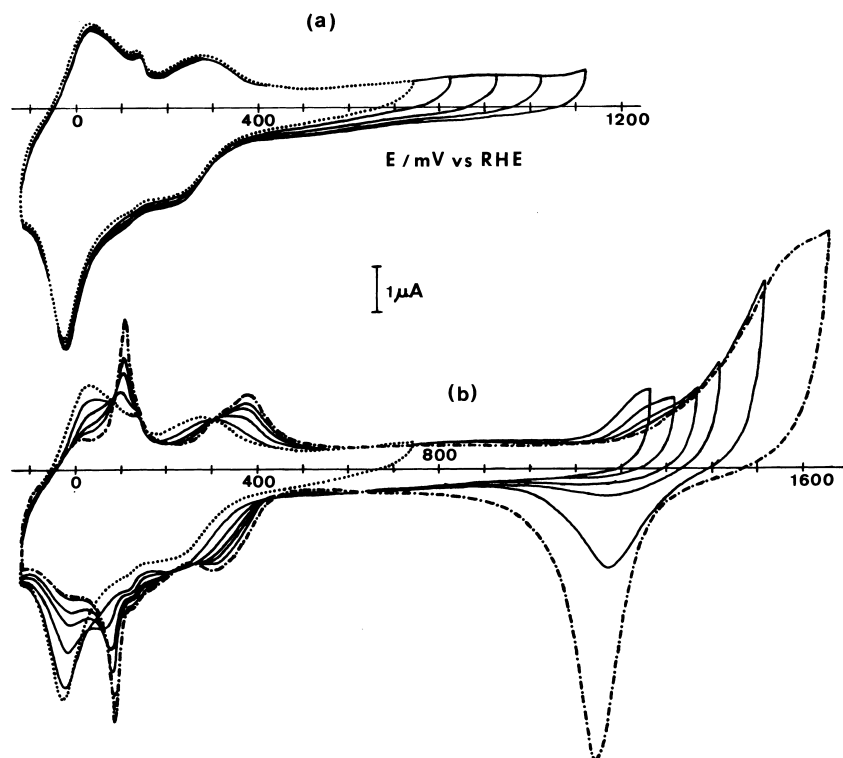
Fig. 2. (a) the CV of the '100'-Au surface in a deaerated 0.01 M HClO$_4$ + 1 mM Pb(II) solution is reproducible provided that the higher vertex potential is within the potential range of '100'-Au stability, (b) increasing the higher vertex potential beyond $\cong$ 1150 mV, gradually changes the CV of '100'-Au to the CV of pc-Au; ($\cdots$) initial CV, ($-\cdot-$) final CV; scan rate 20 mV s^{-1}; rotation rate 9 s^{-1}.

The potentials of bulk deposition, E_{bd}, for $C_{Pb(II)}$ = 1 mM were calculated. We found −105 mV in 0.01 M HClO$_4$ (activity $a(Pb^{2+})$ = 6.6 × 10^{-4} M and E^0 (Pb^{2+}/Pb) = −0.126 V [11]) and 210 mV in 1 M NaOH ($a(HPbO_2^-)$ = 2.5 × 10^{-4} M and E^0 (HPbO$_2^-$/Pb) = −0.54 V [13]). These values agree well with those experimentally observed. Fig. 1 also shows that both E_{bd} and the potential of each peak of the upd spectrum shift 340 mV as the pH goes from 2 to 14. This pH independence of the shift of the potential of each peak as pH changes is a consequence of Pb(II) upd as a neutral atom and leads to the same peak separation (220 mV) at pH 2 and at pH 14 [3].

Upon continuous scanning, a small anodic peak develops at 140 mV in the cyclic voltammogram (CV) of Fig. 1(a) and the peak at 220 mV may shift to 280 mV (cf. Fig. 2(a)).

We previously reported [1] that '100'-Au gradually changes to pc-Au as the potential is cycled to increasingly anodic values beyond the stability limit (≈1150 mV) of the '100-Au' surface. It was not surprising, therefore, to observe that the CV recorded on '100'-Au in 0.01 M HClO$_4$ + 1 mM Pb^{2+} changes to the CV characteristic of a pc-Au surface in the same solution [11] as '100'-Au changes to pc-Au (cf. Fig. 2(a) and (b)). The overall features of the pc-Au CV reveal a somewhat disturbed surface (in the context of what was observed by Hamelin et al. [11]).

3.2. Reduction of O_2 on '100'-Au in a 1 M NaOH + Pb(II) solution

The RDE polarization curves for O$_2$ reduction on '100'-Au recorded in 1 M NaOH containing Pb(II) and restricting the lower potential limit to the onset of lead bulk electrodeposition, are shown in Fig. 3(b). Although they will be further discussed in Section 4.2 in relation to the curves in Fig. 3(a), we stress already here that, relatively to the polarization curves recorded in the absence of Pb(II), (i) the current intensity maximum decreases faster as the rotation rate increases, (ii) at a given rotation rate, the current intensity decrease below the current intensity maximum potential is slower and (iii) beyond 550 mV, the current intensity increases rapidly up to the 4-electron level.

The Koutecky–Levich (K-L) I^{-1} vs. $\omega^{-0.5}$ plots (where ω is the rotation rate) are straight lines (cf. Fig. 4), whereas the plots $I^{0.5}$ vs. $I\omega^{-0.5}$ and I^2 vs.
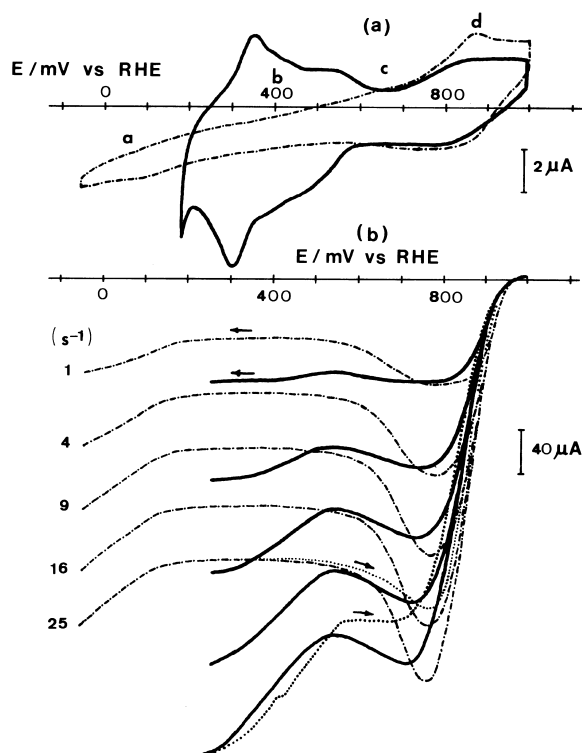
Fig. 3. (a) CVs recorded at 20 mV s^{-1} on a '100'-Au surface in an argon-saturated 1 M NaOH solution and (b) polarization curves recorded at 10 mV s^{-1} on '100'-Au in an O$_2$-saturated 1 M NaOH solution; solutions with (———) and without (– · –) 1 mM Pb(II).

$I\omega^{-0.5}$ are curved (cf. Fig. 5(a) and (b)). As mentioned in Ref. [14], these two plots give a straight line if the reaction order (m) is, respectively, 2 and 0.5. They are mathematically equivalent to the more frequently used $I^{-0.5}$ vs. $I^{0.5}\omega^{-0.5}$ plot for $m = 2$ and I^{-2} vs. $I^{-1}\omega^{-0.5}$ plot for $m = 0.5$; contrarily to them, however, they are generally able to discriminate between reaction orders.

The electroreduction of O$_2$ on '100'-Au in a 1 M NaOH + Pb(II) solution is therefore a first order reaction. From the inverse of the slopes of the I^{-1} vs. $\omega^{-0.5}$ plots, the number of electrons, n, exchanged per O$_2$ molecule reacted was calculated from Eq. (1) [15]:

$$(\text{slope})^{-1} = 0.62nFAD^{2/3}v^{-1/6}C, \qquad (1)$$

where F is the Faraday, A is the electrode area, D and C are, respectively, the diffusion coefficient and the concentration of the reacting species in 1 M NaOH and v is the kinematic viscosity of a 1 M NaOH solution, with $F = 96487$ C mol^{-1}, $D(O_2) = 1.65 \times 10^{-5}$ cm^2 s^{-1} [16], $v = 1.0624 \times 10^{-2}$ cm^2 s^{-1} [17] and $C(O_2) = 8.4 \times 10^{-7}$ mol cm^{-3} [18] and is shown in Fig. 6 relatively to the electrode potential. Below 600
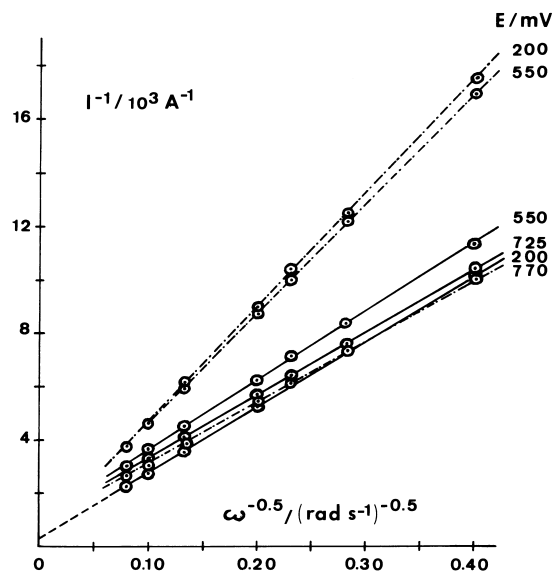

Fig. 4. Koutecky–Levich I^{-1} vs. $\omega^{-0.5}$ plots obtained from the polarization curves of Fig. 3(b); 1 M NaOH solution with (———) and without (– · –) Pb(II).

mV, n is always close to 4 on the '100'-Au surface immersed in the Pb(II) solution, therefore much higher than on '100'-Au in the absence of Pb(II). Below ≈250 mV, the intercepts of the K-L lines are close to the origin.

From the potential of the current intensity maximum down to 550 mV, the Levich plots for '100'-Au in the NaOH + Pb(II) solution curve down as the rotation rate increases (cf. Fig. 7); at the potential of the current intensity maximum, the curvature is higher than that found in the absence of Pb(II) at the same potential.

The rotation independent Tafel slope (cf. Fig. 8) is practically unaltered when Pb(II) is added to the 1 M NaOH solution; it is −60 and −65 mV dec^{-1} for, respectively, in the absence and in the presence of Pb(II). Like the other Tafel slopes reported in this work, these slopes were obtained from a E vs. log($I/I_L - I$) plot (where I and I_L mean, respectively, the disc current intensity and the limiting disc current intensity).

3.3. Reduction and oxidation of HO$_2$- on '100'-Au in a 1 M NaOH + Pb(II) solution

Fig. 9 compares polarization curves obtained on '100'-Au immersed in an argon-saturated 1 M NaOH + 1 mM HO$_2^-$ solution with and without Pb(II). As expected from the data collected for the reduction of O$_2$, the current intensity maximum at 835 mV for HO$_2^-$ reduction decreases when Pb(II) is present in solution. Below 835 mV, the current intensity
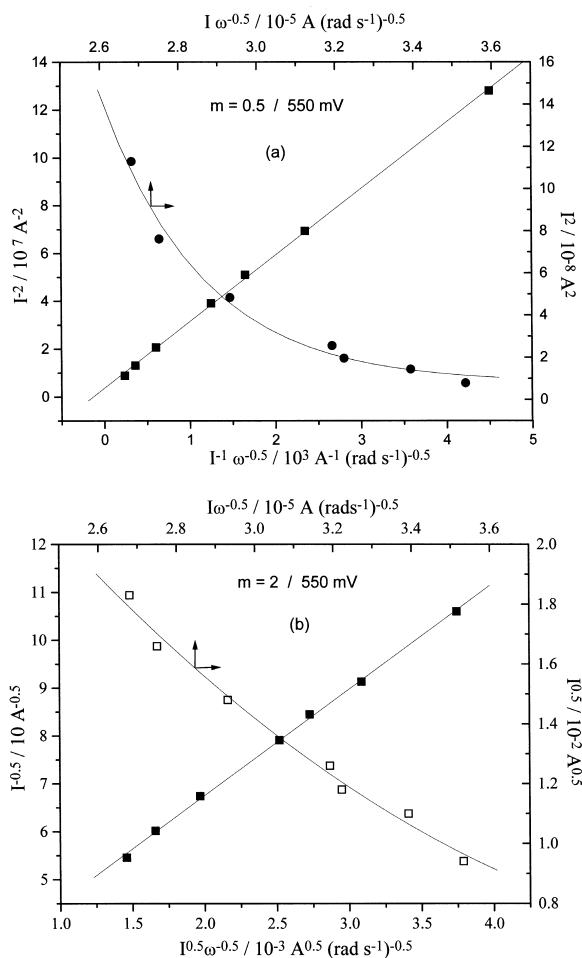
Fig. 5. Comparison between (a) the K-L plots ($-\bullet-$) I^2 vs. $I\omega^{-0.5}$ and ($-\blacksquare-$) I^{-2} vs. $I^{-1}\omega^{-0.5}$ for $m = 0.5$ and between (b) the K–L plots ($-\square-$) $I^{0.5}$ vs. $I\omega^{-0.5}$ and ($-\blacksquare-$) $I^{-0.5}$ vs. $I^{0.5}\omega^{-0.5}$ for $m = 2$ obtained at 550 mV from the polarization curves of Fig. 3(b) for '100'-Au in 1 M NaOH + Pb(II).

decreases both in the presence and in the absence of Pb(II), but the decrease is significantly more gradual when Pb(II) is in solution; by ≈ 200 mV, the current intensity is very small and the same on both experimental situations. Interestingly, however, in the presence of Pb(II) the *decrease* of the HO_2^- reduction current intensity below ≈ 550 mV corresponds to a continuous *increase* of the O_2 reduction current intensity (cf. Fig. 3(b)).

By 200 mV, the HO_2^- reduction current intensity is potential and rotation rate independent both with and without Pb(II) in solution, meaning that it is controlled by a chemical step, most probably HO_2^- disproportionation; the measured current intensity is due to the reduction (under diffusion-controlled conditions) of the O_2 formed in this disproportionation reaction [1].
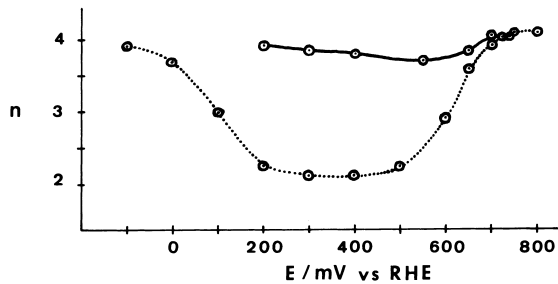

Fig. 6. Plot of the number of electrons exchanged per molecule of O_2 initially reduced as a function of the applied potential; '100'-Au in 1 M NaOH with (——) and without ($\cdots$) Pb(II).

As already found for the same reaction on '100'-Au in the absence of Pb(II) [1], for HO_2^- reduction when Pb(II) is present, (i) the K-L I^{-1} vs. $\omega^{-0.5}$ plots are straight lines, which, together with the curved $I^{0.5}$ vs. $I\omega^{-0.5}$ and I^2 vs. $I\omega^{-0.5}$ plots, means that the reaction is first order; the lines are parallel to each other with a slope corresponding to 2 electrons per HO_2^- reacted calculated from Eq. (1) with $D(HO_2^-) = 8.5 \times 10^{-6}$ cm^2 s^{-1} [19] and $C(HO_2^-) = 1.49 \times 10^{-6}$ mol cm^{-3}, (ii) the rotation independent Tafel slope is -30 mV dec^{-1}, (iii) the Levich plot at 835 mV curves down corresponding to a K-L plot that does not cross the origin.
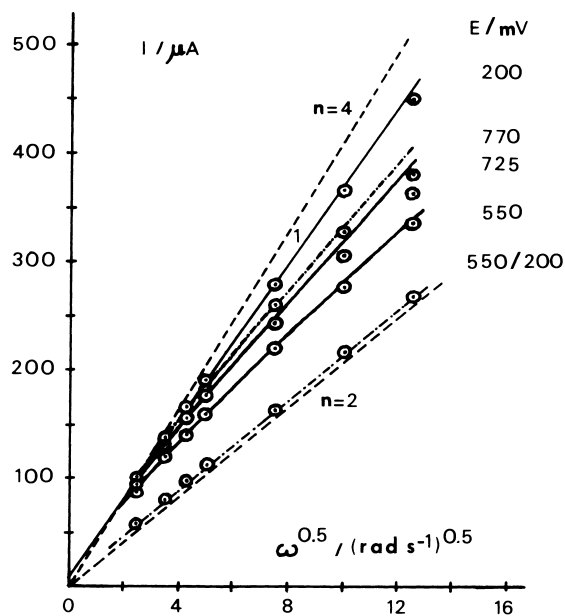

Fig. 7. Levich plots obtained from the polarization curves of Fig. 3(b); 1 M NaOH solution with (———) and without ($-\cdot-$) Pb(II).
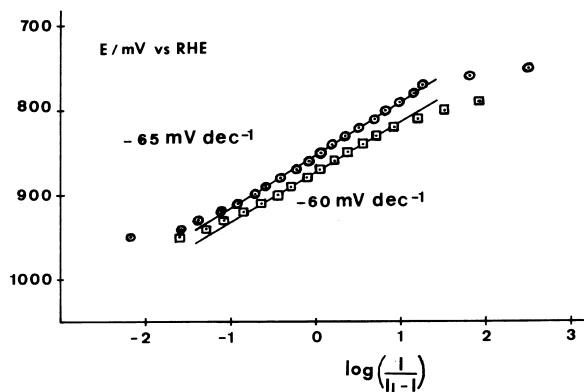
Fig. 8. Tafel slopes obtained from the polarization data in Fig. 3(b); 1 M NaOH solution with $(-\odot-)$ and without Pb(II) (square with dot).

potential. From the slope of that line, the above-mentioned value of $D(HO_2^-)$ was calculated by assuming $n = 2$ in Eq. (1). Less than this number of electrons was found below 1000 mV, probably due to a current intensity decrease as a consequence of the simultaneous reduction of the O_2 produced during the oxidation of HO_2^-.

The observed current intensity for HO_2^- oxidation on '100'-Au in 1 M NaOH is also smaller when Pb(II) is present in solution. The K-L plot at 1050 mV is a straight line that crosses the origin, which means that the oxidation of HO_2^- is diffusion-controlled at that

4. Discussion

4.1. On the nature of the '100'-Au surface

It is not possible to match the observed stripping of lead from '100'-Au with any of the stripping spectra of lead for the Au planes (including (100)) in a 0.01 M $HClO_4$ + 1 mM Pb^{2+} reported by Hamelin et al. (cf. Fig. 1(a) with Fig. 1 of Ref. [3]). We tried, therefore, to rationalise the individual features of the CV of Fig. 1(a)) since only for the upd and stripping peaks of lead in 0.01 M $HClO_4$ there are some data available.

As far as we know, the broad peak at 220 mV was never reported in literature. It may be related to the
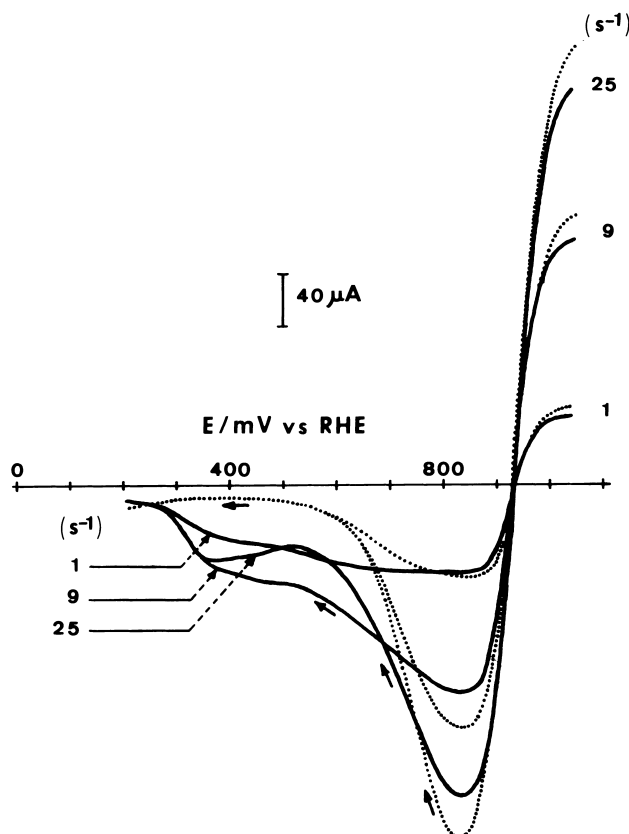

Fig. 9. Polarization curves recorded at 10 mV s^{-1} on a '100'-Au surface in an argonsaturated 1 M NaOH + 1.5 mM HO_2^- solution with (———) and without (· · ·) 1 mM Pb(II).

stripping of lead from narrow terraces on a surface about 18° from the (100) plane on the (100)–(110) zone [20]. The stripping peak at 10 mV is common to pc-Au and to '100'-Au (cf. Fig. 2(b)), although smaller in the CV of pc-Au. In her work on lead upd on pc-Au from a 0.01 M $HClO_4$ + 1 mM Pb^{2+} solution [11], this peak was ascribed by Hamelin to lead deposition on the (311) plane. Later, she related the peak at ≈10 mV observed in the CV of (311) in the same solution to the existence of terraces with (111) orientation and less than four atoms wide [4]. The peak at ≈140 mV may also be related to the (311) plane (cf. Fig. 6 of Ref. [4]). But the CV of '100'-Au in contact with Pb(II) *does not show* the large and reversible peak centered at ≈360 mV observed in the CV of (311) and ascribed by Hamelin to the occurrence of monoatomic steps *with* (100) *orientation* (cf. Fig. 1(a) with Fig. 6 in Ref. [4]). Even if it is accepted that the '100'-Au surface expose (311) planes to the electrolyte, their amount does not appear to be significant. In fact, (i) the only common features between the CV of (311) and the CV of '100'-Au in 0.01 M $HClO_4$ + 1 mM Pb^{2+} are the peaks at 10 mV and at 140 mV; additionally, a peak at 220 mV is observed with '100'-Au but not with (311), whereas a peak at ≈400 mV, which is a characteristic feature of the (311) CV [4], is absent in the CV of '100'-Au, (ii) the '100'-Au surface is more active for O_2 and for HO_2^- electroreduction than (311) [21], (iii) the shapes of the polarization curves for O_2 and for HO_2^- electroreduction on '100'-Au [1] and on (311) [21] are different. Instead, the polarization curves for O_2 reduction on '100'-Au are entirely similar to those recently reported for (100) [22], (iv) for (311), the HO_2^- reduction current intensity in the potential range of the maximum was reported to be smaller in the cathodic scan than in the anodic scan [20] whereas, for '100'-Au, the inverse has always been observed to be true. This difference in hysteresis may indicate that different surface species are present on the two surfaces.

It also appears that the (100)-like behavior of '100'-Au towards O_2 reduction is not due to the presence on the surface of sufficient large number of areas with (100) orientation. Indeed, (i) the CV of '100'-Au does not show *any* of the five peaks associated with the stripping of lead from the (100) surface [20]. Instead and as discussed above, it shows features that may be related to the presence on the '100'-Au surface of planes at 25° (the (311) plane) and at 18° from (100) on the (100)–(110) zone (cf. Fig. 2 of Ref. [20]). However, the peak at ≈400 mV, always present on these planes and ascribed to the stripping of lead from steps [20], is never observed in the CV of '100'-Au, (ii) as we demonstrate below, the behavior towards the electroreduction of O_2 of the '100'-Au surface in the

presence of Pb(II) differs entirely from that reported in the literature for (100) in the same conditions [6, 23].

4.2. Analysis of O_2 reduction on '100'-Au in a 1 M NaOH + Pb(II) solution

In a previous work from this laboratory [1], the discussion of the surface electrochemistry of '100'-Au was based on the electrochemical activity of four surface species (which we referred to by the letters a–d) and these species were related to the way how the surface deals with HO_2^- below 950 mV. The potential ranges of species a to d are indicated in Fig. 3(a), which also compares the CVs of '100'-Au in the absence and in the presence of Pb(II). The CV in the absence of Pb(II) is tilted. Such tilt is not due to the reduction of residual O_2 in the solution, since no change of the current intensity was observed when the electrode was rotated at a significantly high rate. A similar tilted CV was also reported for the (100) plane in alkaline solution [22, 24, 25].

Fig. 3(a) shows that, in the presence of Pb(II), the following changes occur in the CV of '100'-Au:

(i) In the potential range of species d (750–950 mV) and c (600–750 mV), the charge under the anodic and the cathodic peak decreases. Species d results from OH^- adsorption with full charge transfer and was called AuOH [1]. If the potential of zero charge (pzc) of '100'-Au is close to the pzc of pc-Au (≈700 mV [6]), above this potential and in the presence of $HPbO_2^-$ the adsorption of this anion is also possible. We suggest that the discharged OH has to compete with $HPbO_2^-$ for '100'-Au and that, as a result, a certain amount of negative charge builds on this surface. It is also reasonable to accept that this amount of charge decreases as the potential is made more cathodic and the onset of the upd process is approached, due to a partial discharge of the adsorbed $HPbO_2^-$ together with the decrease of its coverage.

(ii) Below 600 mV, the charge under the CV increases due to the upd and to the stripping of lead. These processes occur within the potential regions of species b (300–550 mV) and of species a (50–250 mV).

There are, therefore, essentially two processes that we expect may influence the reduction of O_2 on '100'-Au in 1 M NaOH in the presence of Pb(II): the adsorption of $HPbO_2^-$ and the deposition of Pb adatoms.

4.2.1. Potential range of Pb(II) adsorption

The Levich plots for HO_2^- reduction and for O_2 reduction on '100'-Au at the potential of the maximum (≈800 mV) curve down as the rotation rate increases. This was taken in Ref. [1] as an indication that, at that potential, HO_2^- is disproportionated and that the HO_2^- 'reduction' current is in fact a catalytic current result-

ing from the recycling of the O_2 produced in the disproportionation reaction. It was also proposed that, whereas species d promotes this reaction (by favoring HO_2^- adsorption), change from species d to c decreases its rate constant and, consequently, gives rise to a decrease of the measured current intensity in the potential region of species c. This proposition implies that adsorption (not coadsorption) of HO_2^- on the '100'-Au surface already covered by adsorbed OH species is assumed to occur. The basis for this assumption is the following reasoning: in experiments involving a deaerated 1 M NaOH + HO_2^- solution, HO_2^- is directly available to interact with the electrode after diffusion from solution, whereas in experiments involving an O_2 − saturated 1 M NaOH solution, the only HO_2^- available is that produced by the reduction of O_2. Nevertheless and as shown by the close similarity of the shape of the respective polarization curves, the O_2 reduction and the HO_2^- processes entirely correspond in the potential regions of species d and c. This fact suggests that HO_2^- 'sees' the same surface in both experimental situations and that this surface may be '100'-Au covered by OH species. Actually, the mechanism by which the disproportionation of HO_2^- is catalyzed by the presence of OH species on the surface is not known. The nature of the surface structure called 'adsorbed OH species' in the literature is not known either.

Fig. 9 shows, that the increment as the rotation rate increases of the HO_2^- reduction current intensity on '100'-Au from the onset of HO_2^- 'reduction' down to the potential of the maximum is smaller in the presence of Pb(II) than in its absence; the polarization curves for O_2 reduction in this potential range follow the same trend (cf. Fig. 3(b)). Below the potential of the maximum, the observed decrease of the HO_2^- reduction current intensity is slower on the '100'-Au surface with adsorbed Pb(11) ('100'-Au + Pb(II)(ads)) than on '100'-Au. (cf. Fig. 9) and, again, the O_2 reduction current intensity follows the same trend (cf. Fig. 3(b)). By comparison with what appears to happen on '100'-Au [1], these facts suggest that, on '100'-Au + Pb(II)(ads) (i) O_2 is reduced only to HO_2^- in the potential range of species d and c; the measured current intensity depends on the fate of the produced HO_2^-, (ii) HO_2^- is disproportionated and the O_2 produced is recycled, (iii) the disproportionation process is catalyzed by a surface OH species (which is perturbed by some adsorbed $HPbO_2^-$), (iv) the disproportionation rate constant is lower in the potential range of species d and higher on the potential range of species c.

McIntyre described the disproportionation of HO_2^- catalyzed by surface OH species by Eqs. (2) and (3) [26]

$$HO_2^{-*} + AuOH \longrightarrow OH^- + AuO_2H, \qquad (2)$$

$$AuO_2H + HO_2^{-*} \longrightarrow AuOH + O_2^* + OH^-, \qquad (3)$$
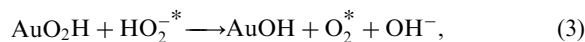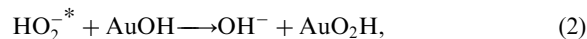
where (*) means vicinity of the electrode surface. He developed the following equations to quantitatively describe the limiting current intensity obtained when O_2 is reduced by a regenerative mechanism involving HO_2^- disproportionation according to Eqs. (2) and (3) and with total rate constant K_4 [26]

$$I_L = 2FAZ_1C_1\omega^{0.5} + 2FAZ_1C_1\omega^{0.5}[K_4/(Z_2\omega^{0.5} + K_4)], \qquad (4)$$

$$I_L = 4FAZ_1C_1\omega^{0.5} - FAZ_2^2\omega/K_4[(1 + 4Z_1C_1K_4/Z_2^2\omega^{0.5}))^{0.5} - 1], \qquad (5)$$

where $Z = 0.62D^{2/3}v^{-1/6}$ and subscripts 1 and 2 refer, respectively, to O_2 and HO_2^-. Depending on which of the two Eq. (2) or Eq. (3), is slower, disproportionation appears, respectively, either as a pseudo-first order (Eq. (4)) or a second order (Eq. (5)) reaction.

As mentioned above, the Levich plot at the potential of the current intensity maximum for O_2 reduction on '100'-Au in a solution containing Pb(II) curves down as the rotation rate increases (cf. Fig. 7). This plot was modelled by applying McIntyre's model and the values of K_4 that gave the best fit to the experimental values of the current intensity measured at the potential of the maximum (750 mV) from the polarization curves in Fig. 3(b) assuming first- or second-order disproportionation, are shown in Table 1. First-order disproportionation and $K_4 = 6.7 \times 10^{-3}$ cm s^{-1} gave the best overall fit. For '100'-Au in the absence of Pb(II), the disproportionation was also found to be first-order and, as expected from the above discussion, the calculated value of K_4 was higher ($= 8.5 \times 10^{-3}$ cm s^{-1}). The agreement between experimental and calculated current intensity values is very good at the lower rotation rates both in the absence and in the presence of Pb(II). However, as the rotation rate increases above 16 s^{-1} the experimental values show a negative shift relatively to the calculated ones. This may be due to the fact that above 16 s^{-1} the rate constant $K_D(2) = Z_2\omega^{0.5}$ for the diffusion of HO_2^- to the solution bulk becomes significant relatively to K_4 and, consequently, the amount of HO_2^- disproportionated decreases. The deviations observed in experiments with '100'-Au covered by a 0.3 μ-thick Nafion film in a 1 M NaOH without Pb(II) were, in fact, significantly smaller than those observed on a bare '100'-Au surface [27].

Below the potential of the maximum, disproportionation of HO_2^- by a pseudo first-order disproportionation was also found to occur on '100'-Au + Pb(II)(ads), but K_4 continuously decreases as the potential goes cathodic. At 550 mV, a value of

Table 1
Experimental I_L vs. calculated I_L (in µA) for 1st- and 2nd-order disproportionation of HO_2^- on '100'-Au + Pb(ads)

Rotation rate (s^{-1})	$E = 725$ mV			$E = 550$ mV		
	experimental (µA)	1st order[a]	2nd order[b]	experimental (µA)	1st order[c]	2nd order[d]
1	96	96	96	89	88	90
2	133	131	133	120	119	124
3	156	157	161	140	141	150
4	176	178	185	160	159	171
9	245	254	270	220	223	247
16	305	323	352	276	282	319
25	364	390	433	336	340	389

[a] $K_4 = 6.7 \times 10^{-3}$ cm s^{-1}.   [b] $K_4 = 3.0 \times 10^4$ cm^4 mol^{-1} s^{-1}.   [c] $K_4 = 3.0 \times 10^{-3}$ cm s^{-1}.   [d] $K_4 = 1.0 \times 10^4$ cm^4 mol^{-1} s^{-1}.

$K_4 = 3.0 \times 10^{-3}$ cm s^{-1} was calculated; in this case, the negative shift of the experimental values is much smaller (cf. Table 1 and Fig. 7). In agreement with that reported in Ref. [1], in the absence of Pb(II) and at the same potential a true first order disproportionation [26] was found to occur (cf. Fig. 7).

The following mechanism

$$HO_2^- \leftrightarrow HO_2^-(^*) \tag{6}$$

$$HO_2^-(^*) \longrightarrow \tfrac{1}{2}O_2(^*) + OH^-, \tag{7}$$
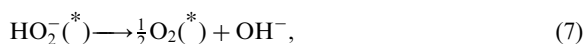
where Eq. (7) is the sum of Eqs. (4) and (5), also assumes that the process of HO_2^- 'reduction' on '100'-Au + Pb(II)(ads) in 1 M NaOH occurs in the potential region of species d and c through the disproportionation of the HO_2^- that diffuses into the vicinity of the electrode; the produced O_2 is then reduced back to HO_2^-. If the reduction of O_2 to HO_2^- is reversible below the potential of the maximum and both the rate constant for this reduction (K_2) and K_4 do not change appreciably in the Tafel potential range, this mechanism predicts the observed Tafel slope of −30 mV dec^{-1}.

4.2.2. Potential range of Pb(II) upd

The reduction of HO_2^- on the '100'-Au surface covered with adsorbed Pb atoms ('100'-Au + Pb(ads)) is significantly dependent on their different states of adsorption. The formation of the first structure of the underpotential-deposited lead causes the decrease of the HO_2^- reduction current intensity to have an halt (cf. Fig. 10); the rapid decrease of this current intensity as the rotation rate increases means that HO_2^- disproportionation still occurs, although with a smaller rate constant than that occurring at higher potentials. The decrease of the HO_2^- reduction current intensity goes on when the second ($\approx$450 mV) and the third structure ($\approx$300 mV) of Pb atoms form; by $\approx$250 mV, the reduction current intensities for '100'-Au + Pb(ads) and for '100'-Au are indistinguishable and very small.

However, the polarization curve for O_2 reduction on '100'-Au + Pb(ads) do not follow this overall decrease of the HO_2^- reduction current intensity. Instead (cf. Fig. 3(b)), below the onset of lead upd the O_2 reduction the current intensity increases continuously (following the increase of the adatoms coverage) from a level corresponding to 3.7 electrons per O_2 molecule
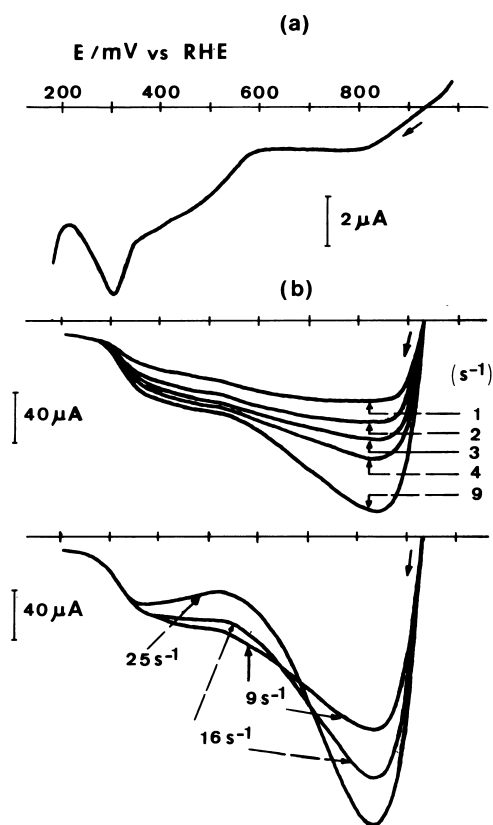

Fig. 10. Cathodic current intensities recorded on '100'-Au in argon-saturated 1 M NaOH + Pb(II) without (a) and with (b) 1.5 mM HO_2^-, scan rates (a) 20 mV s^{-1}, (b) 10 mV s^{-1}.

at 550 mV to the 4-electron level at 250 mV; however, the surface does not show any significant ability to reduce or disproportionate HO_2^- in that potential range. It appears therefore that, below 550 mV, the HO_2^- produced during the reduction of O_2 adsorbs on the '100'-Au + Pb surface in such a way that it is reduced to OH^- before it desorbs and diffuses to the solution bulk.

As mentioned in Section 3.2, although the polarization curves for O_2 reduction show a current intensity plateau below 250 mV, the intercepts of the K-L lines, yet small, do not cross the origin in this potential range and the points of the corresponding Levich plots show an increasingly negative shift relative to the 4-electron Levich lines as the rotation rate increases. Therefore, it appears that, below 250 mV, part of the current intensity is due to an activation-controlled process; this process may be the very slow chemical disproportionation of some of the HO_2^-.

5. Conclusions

The electrochemistry of the '100'-Au surface in a deaerated, alkaline solution containing Pb(II) that this paper reports and discusses, differs considerably from that reported in the literature for the (100) crystallographic orientation of gold in the same experimental conditions. As a result, the way how the lead-modified '100'-Au 'sees' the O_2 molecule is also significantly different from that reported for the (100) gold face.

These facts suggest that there are no significant (100) spots on '100'-Au and that this surface is structurally different from the (100) plane. The only common aspect of the electrochemical behavior of the (100) and the '100'-Au surfaces appears to be the ability to adsorb OH^- with total charge transfer in the potential range of 750 to 950 mV.

References

[1] C. Paliteiro, Electrochim. Acta 39 (1994) 1633.

[2] J. Brooker, P.A. Christensen, A. Hamnett, R. He, C. Paliteiro, Farad. Discuss. 94 (1992) 339.

[3] A. Hamelin, J. Lipkowski, J. Electroanal. Chem. 171 (1984) 317.

[4] A. Hamelin, J. Electroanal. Chem. 165 (1984) 167.

[5] R.R. Adzic, A.V. Tripkovic, N.M. Markovic, J. Electroanal. Chem. 114 (1980) 37.

[6] J.D.E. McIntyre, W.F. Peck, in: J.D.E. McIntyre, M.J. Weaver, E.B. Yeager (Eds.), The Chemistry and Physics of Electrocatalysis, The Electrochernical Society, Princeton, 1984.

[7] M. Alvarez-Rizatti, K. Jüttner, J. Electroanal. Chem. 144 (1983) 351.

[8] K. Jüttner, Electrochim. Acta 29 (1984) 1597.

[9] M. Alvarez, K. Jüttner, Electrochim. Acta 33 (1988) 33.

[10] D.A. Rand, R. Woods, J. Electroanal. Chem. 31 (1971) 29.

[11] D.D. Perrin, W.L.F. Almerego, D.D. Perrin, Purification of Laboratory Chemicals, Pergamon Press, Oxford, 1980.

[12] A. Hamelin, A. Katayama, G. Picq, P. Vennereau, J. Electroanal. Chem. 113 (1980) 293.

[13] Ju. Lurie, Handbook of Analytical Chemistry, Mir Publishers, Moscow, 1975.

[14] C. Paliteiro, Port. Electrochim. Acta 7 (1989) 471.

[15] V.G. Levich, Physicochemical Hydrodynamics, Prentice-Hall, Englewood Cliffs, NJ, 1962.

[16] K.E. Gubbins, R.D. Walker, J. Electrochem. Soc. 112 (1985) 459.

[17] E.W. Washburn, International Critical Tables, vol. 5, McGraw-Hill, New York, 1929.

[18] R.E. Davies, G.L. Horvath, C.W. Tobias, Electrochim. Acta 12 (1967) 287.

[19] F. Van den Brink, W. Visscher, E. Barendrecht, J. Electroanal. Chem. 172 (1984) 301.

[20] A. Hamelin, A. Katayama, J. Electroanal. Chem. 117 (1981) 221.

[21] N.A. Anastasijevic, S. Strbac, R.R. Adzic, J. Electroanal. Chem. 240 (1988) 239.

[22] S. Strbac, N.A. Anastasijevic, R.R. Adzic, J. Electroanal. Chem. 323 (1992) 179.

[23] R.R. Adzic, N.M. Markovic, J. Electroanal. Chem. 138 (1982) 443.

[24] A. Hamelin, M.J. Sottomayor, F. Silva, S.-C. Chang, M.J. Weaver, J. Electroanal. Chem. 295 (1990) 291.

[25] S. Strbac, A. Hamelin, R.R. Adzic, J. Electroanal. Chem. 362 (1993) 47.

[26] J.D. McIntyre, J. Phys. Chem. 71 (1967) 1196.

[27] C. Paliteiro, M.L. Pereira, in: A.J.L. Pombeiro, J.A. McCleverty (Eds.), Molecular Electrochemistry of Inorganic, Bioinorganic and Organometallic Compounds, Nato ASI Series, Kluwer Academic Publishers, Dordrecht, 1993, p. 405.